

CNS-Obsidian: A Neurosurgical Vision-Language Model Built From Scientific Publications

Authors: Anton Alyakin^{1,2,3,*}, Jaden Stryker¹, Daniel Alexander Alber^{1,4}, Jin Vivian Lee², Karl L. Sangwon^{1,4}, Brandon Duderstadt⁵, Akshay Save¹, David Kurland¹, Spencer Frome^{1,4}, Shrutika Singh¹, Jeff Zhang^{1,6,7}, Eunice Yang^{1,8}, Ki Yun Park^{2,3}, Cordelia Orillac¹, Aly A. Valliani¹, Sean Neifert¹, Albert Liu¹, Aneek Patel¹, Christopher Livia¹, Darryl Lau¹, Ilya Laufer¹, Peter A. Rozman¹, Eveline Teresa Hidalgo¹, Howard Riina^{1,9}, Rui Feng¹⁰, Todd Hollon¹¹, Yindalon Aphinyanaphongs^{6,7}, John G. Golfinos^{1,12}, Laura Snyder¹³, Eric C. Leuthardt², Douglas Kondziolka^{1,14}, Eric Karl Oermann^{1,9,15,16,†}

Affiliations:

¹Department of Neurological Surgery, NYU Langone Health; New York, 10016, USA.

²Department of Neurosurgery, Washington University in Saint Louis; Saint Louis, MO 63110, USA.

³Washington University School of Medicine; Saint Louis, MO 63110, USA.

⁴New York University Grossman School of Medicine; New York, NY 10016, USA.

⁵Nomic AI, New York; NY 10003, USA.

⁶Department of Population Health, NYU Langone Health; New York, NY 10016, USA.

⁷Division of Applied AI Technologies, NYU Langone Health; New York, NY 10016, USA.

⁸Columbia University Vagelos College of Physicians and Surgeons; New York, NY, USA.

⁹Department of Radiology, NYU Langone Health; New York, NY 10016, USA.

¹⁰Department of Neurosurgery, Mount Sinai Health System; New York, NY 10019, USA.

¹¹Department of Neurosurgery, University of Michigan; Ann Arbor, MI 48109, USA.

¹²Department of Otolaryngology - Head and Neck Surgery, NYU Langone Health; New York, NY 10016, USA.

¹³Department of Neurosurgery, Barrow Neurological Institute; Phoenix, AZ 85013, USA.

¹⁴Department of Radiation Oncology, NYU Langone Health; New York, NY 10016, USA.

¹⁵Center for Data Science, New York University; New York, NY 10011, USA.

¹⁶Neuroscience Institute, NYU Langone Health; New York, NY 10016, USA.

***Corresponding author (during review):** Anton.Alyakin@nyulangone.org

†Corresponding author (post-review): Eric.Oermann@nyulangone.org

One Sentence Summary: A vision-language model trained on neurosurgical journals matched GPT-4o in clinical diagnosis while advancing scientific publishing and education.

Background

While general-purpose vision-language models (VLMs) demonstrate impressive capabilities, their opaque training on uncurated internet data, undisclosed datasets, and inability to be audited for quality or bias pose critical limitations for high-stakes decision-making settings, such as neurosurgery. We present CNS-Obsidian, a domain-specific VLM trained on peer-reviewed neurosurgical literature, and assess its clinical utility compared with GPT-4o in a real-world setting.

Methods

We processed 23,984 articles from three Congress of Neurological Surgeons journals (*Neurosurgery*, *Operative Neurosurgery*, and *Neurosurgery Practice*), yielding 78,853 figures with captions and in-text mentions. Using GPT-4o and Claude Sonnet-3.5, we converted these image-text pairs into 263,064 training samples across three formats: instruction fine-tuning (127,076), multiple-choice questions (89,587), and differential diagnosis tasks (46,401). We fine-tuned the 34-billion parameter LLaVA-Next model using a three-stage curriculum on 104 H100 GPUs. In a blinded, randomized deployment trial at NYU Langone Health (Aug 30–Nov 30, 2024), neurosurgical clinicians were assigned to use either CNS-Obsidian or a HIPAA-compliant GPT-4o endpoint as diagnostic co-pilots after patient consultations. Primary outcomes were diagnostic helpfulness and diagnostic accuracy, assessed via user ratings and presence of the correct diagnosis within the LLM-provided differential, respectively.

Findings

CNS-Obsidian matched GPT-4o on held-out synthetic questions (76.13% vs 77.54%, $p=0.235$), but only achieved 46.81% accuracy on human-generated multimodal neurosurgery questions versus GPT-4o's 65.70% ($p<10^{-15}$). In the randomized trial, 70 consultations were evaluated (32 CNS-Obsidian, 38 GPT-4o) from 959 total consults (7.3% utilization). CNS-Obsidian received positive ratings in 40.62% of cases versus 57.89% for GPT-4o ($p=0.230$). Both models included the correct diagnosis in approximately 60% of cases (59.38% vs 65.79%, $p=0.626$).

Interpretation

Domain-specific VLMs trained on curated scientific literature can approach frontier model performance in specialized medical domains despite being orders of magnitude smaller. However, low clinical utilization suggests that current chatbot interfaces may not align with diagnostic clinical workflow, at least that of specialists. Future work should explore alternative AI integration strategies beyond conversational interfaces to better support clinical decision-making.

Introduction

The integration of generative artificial intelligence (AI) into neurosurgery holds transformative potential for improving clinical workflows, decision-making, and patient outcomes.¹ Recent pilot studies demonstrated this promise across multiple domains. In evaluating neurosurgical knowledge, a comprehensive assessment of 28 large language models (LLMs) on 2,904 CNS-SANS text-based board examination questions found that 6 models achieved board-passing outcomes, demonstrating the capability of AI to match neurosurgical expertise.² In streamlining documentation workflows, ChatGPT significantly reduced time for discharge notes and operative report writing compared to traditional hospital documentation methods.³ Although generative AI is increasingly utilized in these proof-of-concept systems, the vast majority (84.3%) of neurosurgery studies implement unmodified, generalistLLMs.¹

While general-purpose LLMs demonstrate impressive capabilities, their opaque training on uncurated internet data and inability to be audited for quality or bias pose critical limitations for high-stakes neurosurgical applications.⁴ Attempts to address these concerns in neurosurgery include AtlasGPT, which uses retrieval-augmented generation (RAG) with 250,000 pages of neurosurgical literature to outperform generalist models on board exam benchmarks.⁵ Yet this approach still relies on the underlying closed-source GPT-4 with its undisclosed training data, is text-only, unable to process the visual information essential to neurosurgical practice, and evaluated on synthetic non-clinical benchmarks.

The emergence of vision-language models (VLMs) represents a paradigm shift in surgical AI. SurgVLM, a QWEN-2.5-based VLM trained on approximately 1.8M surgical images with 7.79M conversations across 16 surgery types, not including neurosurgery, demonstrated superior performance compared to out-of-the-box generalist models like GPT-4.0 and Gemini 2.0, achieving one-fold or more increase in performance on complex tasks requiring temporal analysis.⁶ While important and promising change, such models require massive datasets that may not be readily available for specialized fields, such as neurosurgery.

A critical factor in generative AI performance is its training data, often sourced from the Internet. Many AI-driven scientific advancements, such as AlphaFold⁷, rely on domain-specific datasets meticulously curated by the scientific community. However, assembling large, verified, and well-curated scientific datasets remains a challenge, particularly for multimodal applications in specialized fields. We demonstrate how domain-specific foundation models can be developed using high-quality, vision-language datasets derived from peer-reviewed literature. Our approach addresses both challenges: the need for transparent, verifiable training data and the lack of visual reasoning capabilities in neurosurgery-specific models.

In this study, we built a vision-language training dataset from figures and text of neurosurgical articles in the *Neurosurgery Publications* journal family. We implemented a novel, three-stage curriculum learning pipeline to fine-tune a 34-billion parameter vision-language model. Our resulting model, CNS-Obsidian, was deployed as a diagnostic co-pilot in a web interface that facilitated blinded comparison to a state-of-the-art generalist baseline, GPT-4o. In a prospective, randomized trial, CNS-Obsidian matched GPT-4o in diagnostic performance. Our work establishes a reproducible framework to train and validate specialty-specific multimodal large language models by relying on well-provisioned datasets from peer-reviewed scientific literature. (**Fig. 1**)

MATERIALS AND METHODS

Study Design

This study was approved by the NYU Langone Institutional Review Board (i23-00510); the need for informed consent was waived. The study was not pre-registered, as it evaluated user interactions with artificial intelligence (AI) tools post-patient assessment without any influence on real-time decision-making. The tools were not accessible to users during patient interactions (see **Supplementary Text: User Manual and Trial Protocol**). The protocol was reviewed and approved by the leadership of *Neurosurgery Publications* and

Wolters Kluwer. *Self-Assessment of Neurological Surgery* (SANS) questions were used with permission from the CNS.

Data Acquisition and Processing

We developed a pipeline to extract data from three neurosurgical journals: *Neurosurgery* (n=21,219 articles), *Operative Neurosurgery* (n=2,618 articles), and *Neurosurgery Practice* (n=147 articles). We used AWS Textract to detect figures and captions locations and generate bounding boxes for cropping. A regex-based caption matcher then paired images with their corresponding captions using geometric distance calculations from a list of candidates. We extracted a total of 78,853 figures. We used Meta's Nougat⁸ to extract the remaining unstructured texts from the PDFs. We were able to extract a total of 139 million words. A regex-based system identified in-text figure mentions within the texts, linked them to corresponding figure captions, and stored the excerpts along with figure metadata.

Knowledge Translation Framework

Image Filtering

We built an image content classification system using a ResNet-50-based classifier⁹ (feature extraction followed by a linear classifier) to categorize 500 manually annotated figures into three classes:

- Patient imaging (CT, MRI, X-ray, angiography)
- Clinical visuals (surgical fields, microscopy, anatomical drawings)
- Technical content (flowcharts, survival curves, tables)

We extracted the last layer of ResNet features from 400 images to train a linear classifier before validating its performance on the remaining 100 images (**Fig. S1**). We applied this model to filter the rest of the dataset. All conversion candidates underwent an initial filtering step, requiring >100 characters of associated text (combined caption and in-text mentions) for inclusion. For differential diagnosis dataset candidates, patient imaging was differentiated from everything else. For image-to-multiple choice question (MCQ) conversion candidates, patient imaging and clinical visuals were grouped and differentiated from technical content. For instruction fine-tuning dataset candidates, all three classes were differentiated from each other.

Conversion Pipeline

We developed an automated pipeline using OpenAI GPT-4o¹⁰ and Anthropic Claude Sonnet-3.5¹¹ to convert specialized domain knowledge into high-quality training data for vision-language models:

1. Instruction fine-tuning (IFT): Conversational question-answer pairs. (127,076 samples, 4.2M tokens)
2. Multiple-choice (MC): Clinical vignettes with answer options (89,587 samples, 3.7M tokens)
3. Differential diagnosis (DDx): One-line case summaries with ranked diagnoses (46,401 samples, 0.4M tokens)

Each generation task used custom system prompts with four randomly sampled few-shot examples from a pool of 10 examples (IFT used LLaVA-Med¹² examples; MC and DDx used manually created examples). Depending on the task, models were prompted to create a user-assistant conversation, a multiple choice question with discussion, or a patient one liner with a differential diagnosis based on the image, caption, and in-text mention. Models were instructed to avoid explicit references to existence of the caption and the in-text mention. The pipeline included the image of the target figure as a byte string in the API call but excluded example figures. We used structured JSON outputs and performed post-hoc manual cleaning of the data (e.g. by fixing JSON format syntax errors and searching for all uses of “In-Text Mention”).

Dataset Visualization

Data Cartography

To visualize differences between our specialty-specific dataset and a public general medicine dataset (PubMed), we embedded the text portion of the IFT dataset with a similarly generated PubMed dataset¹² into a shared two-dimensional space. We used Nomic Embed Text v1¹³, an open-source BERT-like text embedder, to convert unstructured text into 512-dimensional vectors. We then used tSNE (34) for dimensionality reduction.

Finally, we applied HBDSCAN¹⁴ hierarchical clustering to identify the 12 largest clusters. Cluster labels were assigned by sampling representative texts from within and outside each cluster and querying GPT-4o to generate a unifying thematic name based on the extracted content. Comparison of NeuroPubs with PubMed revealed notable gaps in broader AI datasets, such as the underrepresentation of cerebral and spinal imaging content (**Fig. 2**).

Model Architecture and Training

Vision-Language Model Backbone

We chose LLaVA-Next as our pretrained multimodal backbone.¹⁵ Large Language and Visual Assistant (LLaVA) is an autoregressive, multimodal large language model that implements a vision-transformer initialized from CLIP features and aligns embeddings of image and text. That is, during pre-training, it is taught to maximize the similarity of image-text pairs while generating de-novo text via next-token prediction. LLaVA-Next improved this design through multilayer projections, patch-based processing of high-resolution images, and an enhanced pre-training strategy.¹⁵ (**Fig. S2A**) Our starting point was the 34-billion parameter (Nous Hermes 2 Yi-34B language model) checkpoint of LLaVA-Next¹⁵ from Hugging Face Transformers, which was then finetuned on neurosurgery-specific content.

Three-Stage Curriculum Training

Based on the LLaVA-Med medical curriculum training¹², we designed a three-stage fine-tuning protocol for a specialist model (**Fig. S2B**):

- 1) Medical alignment: we kept the language model frozen and trained only the projection layers on PubMed-based figure-caption pairs
- 2) Medical knowledge integration: we trained both projection and language models on general medicine PubMed-based conversations (IFT) dataset generated using GPT-4o.
- 3) Neurosurgical specialization: we maintained the same unfrozen components while training on our domain-specific, Neurosurgery Publications-based, and task-specific (IFT, MC, and DDx) datasets generated using GPT-4o and Claude Sonnet 3.5.

Training Details

Models were trained using 104 H100s GPUs (13 nodes, 8 GPUs each) on NYU Langone’s UltraViolet high-performance computing cluster. PyTorch FSDP was used for training parallelization. We used bfloat16 precision, with learning rates of 1e-3 for Stage 1 and 1e-5 for Stages 2 and 3, and cosine scheduling. Mini-batch size per GPU was four, with a gradient accumulation of four steps during Stage 1, yielding effective batch sizes of 1664 for Stage 1 and 416 for Stages 2 and 3. Similar to LLaVA-Med¹², we froze the vision encoder for training stability. We maintained paper-level data splits, allocating 95% of journal articles for training, and 2.5% each for validation and test sets. The validation set was used to optimize training and guide model selection, while the held-out test set was only used to evaluate our final models.

Training Length

We refer to different checkpoints of our model as [$\langle \# \text{ of Stage 1 epochs} \rangle$, $\langle \# \text{ of Stage 2 epochs} \rangle$, $\langle \# \text{ of Stage 3 epochs} \rangle$] for brevity and convenience. We started with recreating LLaVA-Med’s framework, but using LLaVA-Next architecture, with one epoch of Stage 1 training and three epochs of Stage 2 training, yielding our LLaVA-Next-Med [1, 3, 0]. We initially trained this model on three epochs of GPT-Only Stage 3 datasets, yielding [1, 3, 3]. Through extensive experiments and ablation studies (see **Fig. S3-S5** for results; also see **Supplementary Text: Ablation Experiments**), we found that the standard training duration of one epoch for alignment and three epochs for medical and neurosurgical fine-tuning was insufficient for a model of this scale (**Fig. S3-S4**). Our best performing model ended up being extensively trained [5, 10, 10]. Throughout our training length experiments we only used GPT-sourced data for training. We also experimented with training this model on Claude and GPT-based data together, trying both the constraint for epoch number and compute amount (**Fig. S5**). Wall-clock training time per epoch was 3.5 hours for Stage 1, 30 minutes for Stage 2, and 1

hour for Stage 3 using only one data source (e.g. only GPT-4o) and 2 hours if using both GPT-4o- and Sonnet 3.5-based datasets.

Generative AI Evaluation

Benchmarking

We compared LLaVA-Next-Med and CNS-Obsidian to multiple baselines (LLaVA-Med, base LLaVA-Next, OpenAI GPT-4o, and Anthropic Claude Sonnet 3.5). For our models, LLaVA-Med, as well as LLaVA-Next we used vLLM for deployment and made calls to the deployed model via requests interface. For GPT-4o and Sonnet 3.5 evaluations, we made direct API calls to the publicly available checkpoints. We used a local instance of LLaMA-70B to parse the models' chain-of-thoughts and convert them to single-letter answers for automated matching against ground truth.

Synthetic Benchmarks

Synthetic benchmarks consisted of 1,282 GPT-generated and 1,239 Claude-generated MCQs from the held-out test data (2.5% of the total dataset). Paper-level splitting during training ensured that these test questions did not overlap with previously seen questions or figures from training papers. These synthetic benchmarks were used to guide our decisions in ablation studies.

Human-Made Benchmarks

Human-made benchmarks consisted of 950 image-associated questions from the SANS question bank, developed by the CNS for neurosurgery residents preparing for ABNS. Of the total 3,965 questions provided by the CNS, 950 questions included associated images, which were used as our primary benchmark.

Randomized Controlled Trial

In a controlled comparison of diagnostic accuracy and utility, we randomized clinician participants (neurosurgery physicians and advanced practice providers) to either CNS-Obsidian or a PHI-safe version of GPT-4o. To facilitate this, we developed a full-stack application for automated blinding and randomization. Randomization was performed independently for each patient encounter using Python's SciPy pseudorandomness. The user interface (**Fig. S6**) was adapted from a publicly available framework Chatbot UI, implemented in React and Next.js, and extended with features such as secure authentication, medical reference number recording, image submission, and endpoint randomization for each new session. The system utilized Postgres for account and chat storage, Flask with SQLiteDB for authentication, vLLM for hosting the local model (CNS-Obsidian), and Kong as an API gateway to connect with the PHI-safe OpenAI GPT-4o. The base version of our model, CNS-Obsidian-Base [1, 3, 3], was used throughout the trial.

Data was collected for three months, from August 30th, 2024 to November 30th, 2024, at NYU Langone Health, Tisch Hospital for all completed neurosurgery consultations. All trainees and faculty in the department were invited to participate via email. Participation was voluntary and no compensation was provided. Participants were instructed to interact with the software after finishing an encounter with a consult patient.

Outcomes

Diagnostic Helpfulness

Clinicians submitted medical images alongside concise clinical summaries ("one-liners"). Models were prompted to generate a differential diagnosis in their first response, which clinicians then rated as either clinically helpful ("thumbs up") or not ("thumbs down"). Clinicians could optionally continue the conversation, and follow-up chats involved next-step clinical decision-making queries such as diagnostic workup and best management. The primary outcome of the study was the subjectively rated diagnostic helpfulness of the first response, defined as the frequency of "thumbs up".

Diagnostic Accuracy

For each submitted case, patient identifiers were recorded but omitted from model inputs. Ground truth diagnoses were retrospectively retrieved and compared against model-generated differential diagnoses. Accuracy of the differential diagnosis, measured as the proportion of cases where the true diagnosis appeared in the list of differentials served as an additional primary outcome. Evaluation involved a two-step automated process:

- GPT-4o extracted individual diagnoses from the unstructured model outputs into a structured list.
- GPT-4o determined whether the true diagnosis was included in this list.

During analysis, GPT-4o's differentials were observed to be longer and less specific compared to CNS-Obsidian. To address this, we introduced an ad-hoc adjusted accuracy metric: the correct diagnosis rate per differential, measured as the proportion of total items in the list with a correct diagnosis.

User Engagement

Secondary outcomes included the conversation length and the clinical helpfulness of the follow-up chats. Conversation length was measured as the total number of user messages in the chat per conversation (baseline of 1). Clinical helpfulness of follow-up chats was measured as a binary outcome with upvote or downvote by the user. We also recorded the total number of clinician interactions and total number of neurosurgery consults during the study period.

Statistical Analysis

For generative AI MCQ performance evaluations, two-sided Fisher's exact tests were performed to assess differences in proportions (% accuracy) between models across benchmarking comparisons. The randomized trial was designed to compare differences in subjective (diagnostic helpfulness, clinical helpfulness) and objective (diagnostic accuracy, length-adjusted diagnostic accuracy, conversation length) outcomes between CNS-Obsidian and GPT-4o. Two-sided Fisher's exact tests were performed to assess differences in proportions (all outcomes except conversation length) between models. Two-sided Mann-Whitney U test was performed to assess differences in distributions (conversation length) between models.

RESULTS

Benchmark performance

Performance assessment on MCQ exams showed that CNS-Obsidian matched GPT-4o's accuracy on the held-out GPT-generated MCQs ($p=0.2347$) (**Fig. 3C**) and also outperformed both GPT-4o and Claude Sonnet-3.5 on Claude-generated MCQs ($p=0.0011$ and 0.0004 , respectively), despite being exclusively trained on the GPT-generated data (**Fig. 3D**). Zero-shot accuracy on the human-generated CNS-SANS questions improved from a baseline of 39.81% to 46.81%, but still lagged behind GPT-4o (65.70%, $p<10^{-15}$) (**Fig. 3E**), likely due to data contamination within the frontier models. Adding Claude-generated data to the training set improved accuracy on Claude-generated MCQs ($p=0.0427$) but not performance on GPT-generated MCQs ($p=1.000$) or SANS ($p=0.5193$) (**Fig. 3C-E**).

CNS-Obsidian as a clinical diagnostic co-pilot

During the 92-day trial, a total of 70 chats were generated (0.75/day; 38 randomized to GPT-4o, 32 randomized to CNS-Obsidian) (**Fig. 4A, Fig. S7, Videos S1 and S2**) and 959 total consults seen by neurosurgery (10.42/day), suggesting meaningful but modest AI engagement (7.3% utilization rate). For our primary endpoint (diagnostic helpfulness), CNS-Obsidian achieved a 40.62% upvote rate versus 57.89% for GPT-4o ($p=0.2301$) (**Fig. 4B**). For the secondary endpoint (diagnostic accuracy), CNS-Obsidian included the correct diagnosis at the time of consultation in 59.38% of cases versus GPT-4o did in 65.79% ($p=0.6259$) (**Fig. 4C**). Noting that GPT-4o tended towards broader and lengthier differentials (as exemplified by **Fig. 4A**), we adjusted for response length (i.e., number of correct diagnoses divided by the total number of differentials in the list) and found that CNS-Obsidian non-significantly trended toward a higher correct diagnosis rate per differential than GPT-4o (16.88% vs. 10.69%, $p=0.0809$) (**Fig. 4D**). Users were encouraged to ask follow-up questions such as

further diagnostic work-up or suggested management. For our assessment of user engagement, average conversation length was 2.50 (CNS-Obsidian) versus 1.79 messages (GPT-4o, $p=0.6655$) (**Fig 4E**), with users rating the helpfulness of follow-up conversation lower for CNS-Obsidian than for GPT-4o (upvote rate 25.00% vs. 40.00%, $p=0.2094$) (**Fig. 4F**).

DISCUSSION

We present CNS-Obsidian, a neurosurgical vision-language model trained on a curated dataset of peer-reviewed journal articles. While CNS-Obsidian did not surpass GPT-4o's performance, its development demonstrates critical advantages: transparent and auditable training data from verified sources, domain-specific optimization without the opacity of internet-scraped datasets, and the ability to create specialized models orders of magnitude smaller than frontier models while maintaining clinical utility. There have been previous attempts at using scientific publications to train vision-language models, most of which are non-generative contrastive learning models.^{16–19} Some works have explored converting figure captions to simple visual question-answering datasets using GPT-4o.^{12,20} Importantly, all of these works use the publicly available PubMedCentral-Open Access. During the submission process, we became aware of the work done in parallel to ours²¹ of training the same architecture on a fusion of PubMed¹² and general internet data¹⁵, yielding their version of LLaVA-Next-Med. Unlike models trained on public medical corpora, CNS-Obsidian is the first VLM trained entirely on specialty-specific peer-reviewed literature. Lastly, VLMs have been fine-tuned on scraped medical textbooks,²² but without the use of IFT they are sometimes outperformed even by baseline models. Our work is unique in its data source (peer-reviewed, limited-access journals), implementation and experimentation extensiveness, and the ultimate goal of serving as a clinical co-pilot. Securing explicit permissions from the publishers demonstrates a potential future avenue of ethical and productive symbiotic relationship between AI and scientific publications.

We converted *Neurosurgery Publications*, the journal family of the *Congress of Neurological Surgeons*, into a high-quality AI training and knowledge dataset and used it to build a 34B parameter VLM optimized for differential diagnostic reasoning. Unlike prior LLM-based diagnostic approaches relying on prompt engineering²³ or RAG⁵ we directly fine-tuned our model on curated vision-language cases with differential diagnoses. To ensure rigorous evaluation, we performed a paper-level data split, holding out entire articles from training to minimize potential data contamination. In contrast, the training datasets of GPT-4o and Claude Sonnet-3.5 remain largely unknown, with published instances of data leakage falsely inflating benchmark performance^{24,25}; we believe this to be a rigorous control for potential data contamination. Our findings reinforce the importance of in-domain data, as CNS-Obsidian performed comparably to frontier models like GPT-4o and Claude Sonnet-3.5 on neurosurgical MCQs. Since high-quality medical information is scarce in public datasets¹² and uncurated internet sources such as Twitter²⁶, scientific publications offer an immediate solution, particularly for multimodal paired image-text context, which is rare outside of curated sources.

We conducted the first blinded randomized trial of VLM chatbots in a clinical setting. Unlike prior studies using simulated scenarios^{23,27}, our trial captured the complexities of actual patient care. Neurosurgical residents at a major academic center used a web-based chat interface to interact with a VLM, providing post-encounter, but real-time differential diagnoses. CNS-Obsidian and GPT-4o were perceived as helpful at the point of care nearly half the time, with similar engagement levels. Our clinical deployment was conducted using a checkpoint obtained on August 30th, 2024, while subsequent training improvements were realized after the RCT was underway (**Fig. S3-S5**). This suggests the full point-of-care potential of our model may be underestimated, but points to a greater incongruity between LLM development phases and their prospective validation in long-term clinical deployments.

A key finding was the low utilization rate of the chatbot by neurosurgical participants. We presume that highly trained specialists prefer automation that reduces their workload rather than assists in decision-making. The chatbot interface itself may be a barrier – taking photos and typing responses may be an unnecessary burden for

specialists but could be more useful for generalists and non-specialist practitioners, as the broader scope of their practice makes AI-driven insights more valuable. Additionally, despite the differentials being perceived as helpful, neither model consistently provided the final, official diagnosis.

We acknowledge that our study has limitations. First, we focused on fully autoregressive models, excluding cross-attention-based architectures^{28,29} or grounding strategies that better align text and image features. Second, to ensure compliance with copyright laws and AI-training ethical standards, our dataset was limited to a single journal family, *Neurosurgery Publications*, rather than the full scope of neurosurgical literature. While copyright restrictions prevent sharing CNS-Obsidian's weights, our approach establishes a transparent, ethical framework for using published content with explicit permissions. Though it remains an open question whether models trained on data transformed by other LLMs constitute the same copyrighted knowledge in different textual form, we erred on the side of caution and respect to the publisher. Third, our blinded randomized trial had a low participation rate and was conducted at a single institution, limiting generalizability and emphasizing the need for multicenter studies with larger sample sizes. The low participation rate raises questions about improving human-AI interactions in medicine, echoing findings from a recent study where surgeons in Greece had more negative perceptions of a GPT-4-based chatbot than other physician.³⁰ Alternative interfaces beyond chatbots, such as passive AI-assisted workflows (ambient dictation), may be more aligned with specialist needs. Future studies should explore prompt-based techniques like RAG or chain-of-thought prompting to improve performance.

CONCLUSION

Our work showcases how scientific literature can be leveraged to build powerful, domain-specific AI models. Despite being several orders of magnitude smaller than GPT-4o, our 34B parameter VLM trained on transformed journal content reached acceptable performance on specialty MCQ assessments and as a diagnostic co-pilot. These results highlight the potential for mesoscale VLMs – models built by scientific and medical communities using domain-specific data to meet specialized needs. As AI continues to shape scientific discovery and clinical practice, future research should focus on improving AI-human collaboration, refining training strategies, and developing specialist-friendly interfaces to maximize impact in education and clinical care.

Acknowledgements: We appreciate the informal input from mentors, colleagues, and lab members of OLAB and Leuthardt Lab not individually acknowledged. We thank Michael Constantino, Ali Siavosh-Haghighi, Kevin Yie, and the rest of the NYU Langone High-Performance Computing (HPC) Team, who supported the computing resources fundamental to our work. Lastly, we thank the NYULH Predictive Analytics Unit for their teamwork and collaboration in making AI technologies a reality at NYULH. We also want to thank the *Congress of Neurological Surgeons* and Wolters Kluwer who run and publish *Neurosurgery Publications*, respectively. We would also like to thank the Managing Editor of *Neurosurgery Publications*, Brandon Fiedor, for his tireless work in promoting medical and scientific scholarship.

Funding:

National Cancer Institute’s Early Surgeon Scientist Program grant 3P30CA016087-41S1 (EKO)
W.M. Keck Foundation (EKO)

Author contributions:

Conceptualization and supervision: EKO
Journal publication data collection: AA, JS, KS, DKu
Data extraction, processing, filtering, and organization: AA, JS
Data embedding, mapping, and visualizations: BD
Data conversion pipeline development: AA
Model development and training: AA
Model evaluation suite: JS
Benchmarking and ablations: AA, JS, EKO
Randomized trial user interface and web stack development: JS, EKO
Clinician onboarding to trial interface and patient data provision: AS, CO, AV, SN, AL, AP, CL, IL, DO, DK, EKO
Retrospective assessment of final diagnoses: AS, SF
Statistical analyses of trial data: AA, EKO
Manuscript figure design: AA, DAA, BD, KS, EKO
Manuscript drafting: AA, DA, JVL, EKO
Manuscript revision and final editing: All authors

Competing interests: E.K.O. reports consulting with Sofinnova Partners and Google, income from Merck & Co. and Mirati Therapeutics, and equity in Artisight. R.F., T.C.H., and E.K.O. are editorial board members of *Neurosurgery Publications*. D.K. is the editor in chief of *Neurosurgery Publications*. B.D. is a co-founder and CEO of Nomic AI.

Data and materials availability:

Data used for the general medicine stages of model training was downloaded from the public LLaVA-Med GitHub repository (<https://github.com/microsoft/LLaVA-Med>). Data from *Neurosurgery Publications* was used with permission of the publisher, but will not be released as it is protected by the respective copyrights and trademarks. *Self-Assessment of Neurological Surgery (SANS)* questions were used with permission of the *Congress of Neurological Surgeons (CNS)* and are intellectual property of the *CNS*. Clinical data was collected under a protocol approved by the NYU Langone Institutional Review Board (i23-00510) and is protected by the Health Insurance Portability Accountability Act. Icons were sourced from the Noun Project (<https://thenounproject.com/>).

Code availability:

We used Python 3.10, 3.11, and 3.12, as well as many open-source libraries, including datamapplot 0.4.2, HuggingFace Transformers 4.44.0, matplotlib 3.9.1, numpy 1.26.4, openai 1.55.3, pandas 2.2.0, pillow 10.1.0,

pytorch 2.4, seaborn 0.13.2, wandb 0.17.6, among others. Our training and evaluations were executed using SLURM on the NYU Langone HPC cluster UltraViolet. We used NVIDIA Cuda 12.1. Our data filtering, data conversion, and training code will be publicly released on GitHub (<https://github.com/nyuolab/>) upon publication of this work. The few-shot examples used in the conversion pipelines will be omitted as they use excerpts from the *Neurosurgery Publications* materials. Weights for LLAVA-Next-Med-OLAB are publicly available (<https://huggingface.co/NYU-OLAB/LLaVA-Next-Med-OLAB>). The final CNS-Obsidian model will not be released as it was trained on proprietary content from Wolters Kluwer.

References

1. Patil, A. *et al.* Large language models in neurosurgery: a systematic review and meta-analysis. *Acta Neurochir. (Wien)* **166**, 475 (2024).
2. Vishwanath, K. *et al.* Evaluating the performance and fragility of large language models on the self-assessment for neurological surgeons. *arXiv [cs.CL]* (2025).
3. Dubinski, D. *et al.* Leveraging artificial intelligence in neurosurgery-unveiling ChatGPT for neurosurgical discharge summaries and operative reports. *Acta Neurochir. (Wien)* **166**, 38 (2024).
4. Alber, D. A. *et al.* Medical large language models are vulnerable to data-poisoning attacks. *Nat. Med.* **31**, 618–626 (2025).
5. Ali, R. *et al.* AtlasGPT: a language model grounded in neurosurgery with domain-specific data and document retrieval. *J. Neurosurg.* 1–8 (2025).
6. Zeng, Z. *et al.* SurgVLM: A large vision-language model and systematic evaluation benchmark for surgical intelligence. *arXiv [cs.CV]* (2025).
7. Senior, A. W. *et al.* Improved protein structure prediction using potentials from deep learning. *Nature* **577**, 706–710 (2020).
8. Blecher, L., Cucurull, G., Scialom, T. & Stojnic, R. Nougat: Neural Optical Understanding for Academic Documents. *arXiv [cs.LG]* (2023).
9. He, K., Zhang, X., Ren, S. & Sun, J. Deep residual learning for image recognition. *Proc. IEEE Comput. Soc. Conf. Comput. Vis. Pattern Recognit.* 770–778 (2015).
10. OpenAI *et al.* GPT-4o System Card. *arXiv [cs.CL]* (2024).
11. Claude 3.5 Sonnet. <https://www.anthropic.com/news/claude-3-5-sonnet>.
12. Li, C. *et al.* LLaVA-Med: Training a Large Language-and-Vision Assistant for BioMedicine in one day. *arXiv [cs.CV]* (2023).
13. Nussbaum, Z., Morris, J. X., Duderstadt, B. & Mulyar, A. Nomic embed: Training a reproducible long context text embedder. *arXiv [cs.CL]* (2024).

14. Campello, R. J. G. B., Moulavi, D. & Sander, J. Density-based clustering based on hierarchical density estimates. in *Advances in Knowledge Discovery and Data Mining* 160–172 (Springer Berlin Heidelberg, Berlin, Heidelberg, 2013).
15. Liu, H. *et al.* LLaVA-NeXT: Improved reasoning, OCR, and world knowledge. *LLaVA* <https://llava-vl.github.io/blog/2024-01-30-llava-next/> (2024).
16. Lin, W. *et al.* PMC-CLIP: Contrastive Language-Image Pre-training using Biomedical Documents. *arXiv [cs.CV]* (2023).
17. Zhang, S. *et al.* BiomedCLIP: a multimodal biomedical foundation model pretrained from fifteen million scientific image-text pairs. *arXiv [cs.CV]* (2023).
18. Eslami, S., Meinel, C. & De Melo, G. PubMedCLIP: How much does CLIP benefit visual question answering in the medical domain? *Findings* 1151–1163 (2023).
19. Lozano, A. *et al.* BIOMEDICA: An open biomedical image-caption archive, dataset, and vision-language models derived from scientific literature. *arXiv [cs.CV]* (2025).
20. Zhang, X. *et al.* Development of a large-scale medical visual question-answering dataset. *Commun. Med. (Lond.)* **4**, 277 (2024).
21. Guo, Y. & Huang, W. LLaVA-NeXT-med: Medical multimodal large language model. in *2025 Asia-Europe Conference on Cybersecurity, Internet of Things and Soft Computing (CITSC)* 474–477 (IEEE, 2025).
22. Moor, M. *et al.* Med-flamingo: A multimodal medical few-shot learner. *arXiv [cs.CV]* (2023).
23. McDuff, D. *et al.* Towards accurate differential diagnosis with large language models. *Nature* (2025) doi:10.1038/s41586-025-08869-4.
24. Nori, H., King, N., McKinney, S. M., Carignan, D. & Horvitz, E. Capabilities of GPT-4 on medical challenge problems. *arXiv [cs.CL]* (2023).
25. Deng, C., Zhao, Y., Tang, X., Gerstein, M. & Cohan, A. Investigating data contamination in modern benchmarks for large language models. in *Proceedings of the 2024 Conference of the North American Chapter of the Association for Computational Linguistics: Human Language Technologies (Volume 1:*

Long Papers) (Association for Computational Linguistics, Stroudsburg, PA, USA, 2024).

doi:10.18653/v1/2024.naacl-long.482.

26. Huang, Z., Bianchi, F., Yuksekogonul, M., Montine, T. J. & Zou, J. A visual-language foundation model for pathology image analysis using medical Twitter. *Nat. Med.* **29**, 2307–2316 (2023).
27. Tu, T. *et al.* Towards conversational diagnostic artificial intelligence. *Nature* (2025)
doi:10.1038/s41586-025-08866-7.
28. Alayrac, J.-B. *et al.* Flamingo: A visual language model for few-shot learning. *Adv. Neural Inf. Process. Syst.* **abs/2204.14198**, (2022).
29. Dai, W. *et al.* NVLM: Open Frontier-Class Multimodal LLMs. *arXiv [cs.CL]* (2024).
30. Triantafyllopoulos, L. *et al.* Evaluating the interactions of Medical Doctors with chatbots based on large language models: Insights from a nationwide study in the Greek healthcare sector using ChatGPT. *Comput. Human Behav.* **161**, 108404 (2024).

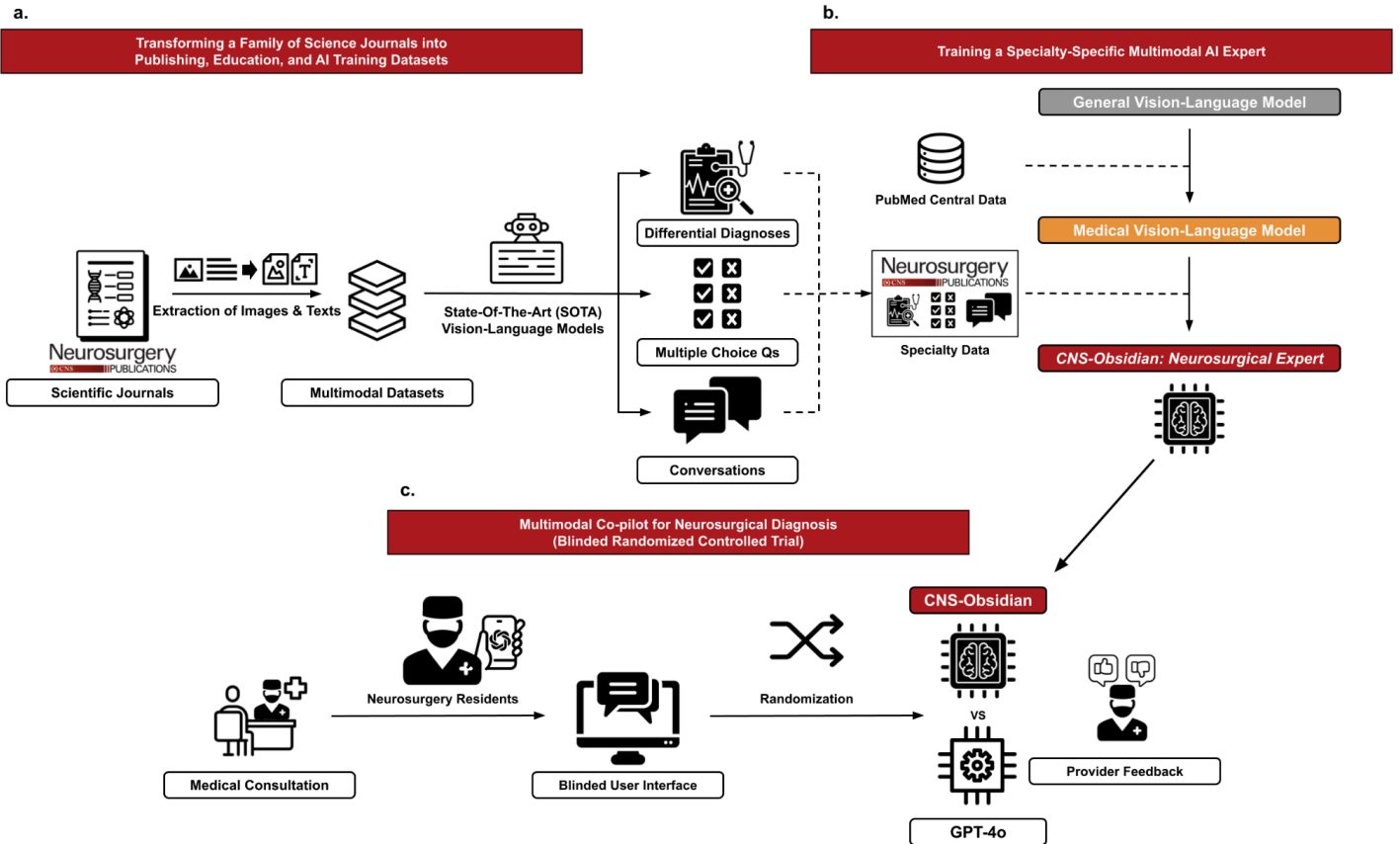


Fig. 1. Overview of key contributions. (A) We developed a pipeline for the acquisition, extraction, and filtering of figures, captions, and in-text mentions from a family of biomedical journals. We converted this data from unstructured biomedical texts and images into publication-, education-, and task-specific AI training datasets. (B) We trained CNS-Obsidian, a 34B parameter autoregressive vision-language model, to be tailored to domain-specific needs for neurosurgery by implementing a novel training step designed to specifically entrain capabilities in differential diagnosis while maintaining the ability to converse and answer questions. (C) We conducted a blinded, randomized, controlled trial comparing CNS Obsidian to GPT-4o as diagnostic copilots on a busy inpatient surgical service.

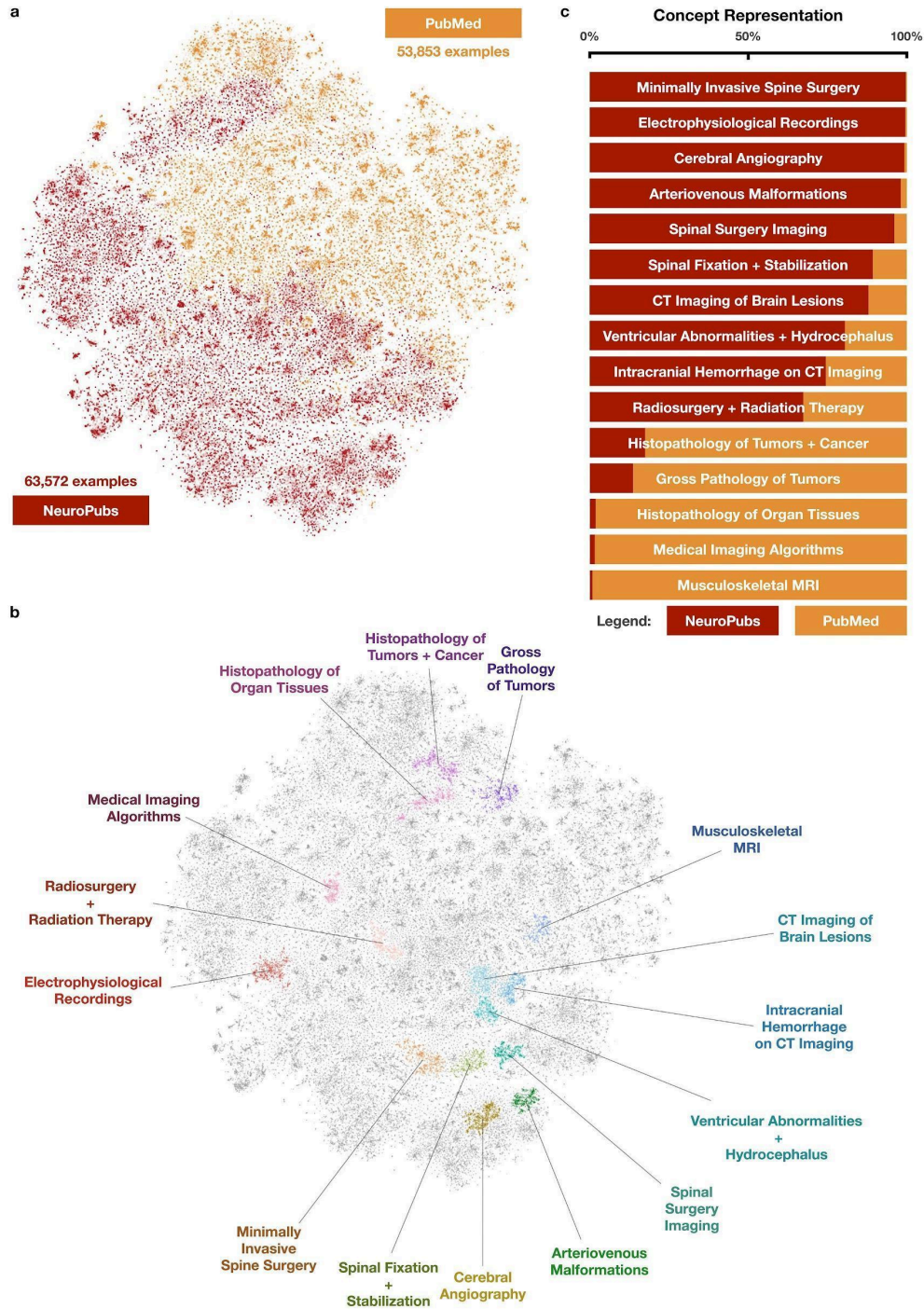


Fig. 2. Visualization of concepts represented in scientific datasets. (A) A joint embedding of the PubMed-based and Neurosurgery-based instruction fine-tuning datasets. (B) The 15 largest hierarchical clusters of the joint embedding. (C) Comparison of the percent composition of the 15 largest clusters in the datasets. NeuroPubs is particularly dense in the highly-specialized neurosurgical topics.

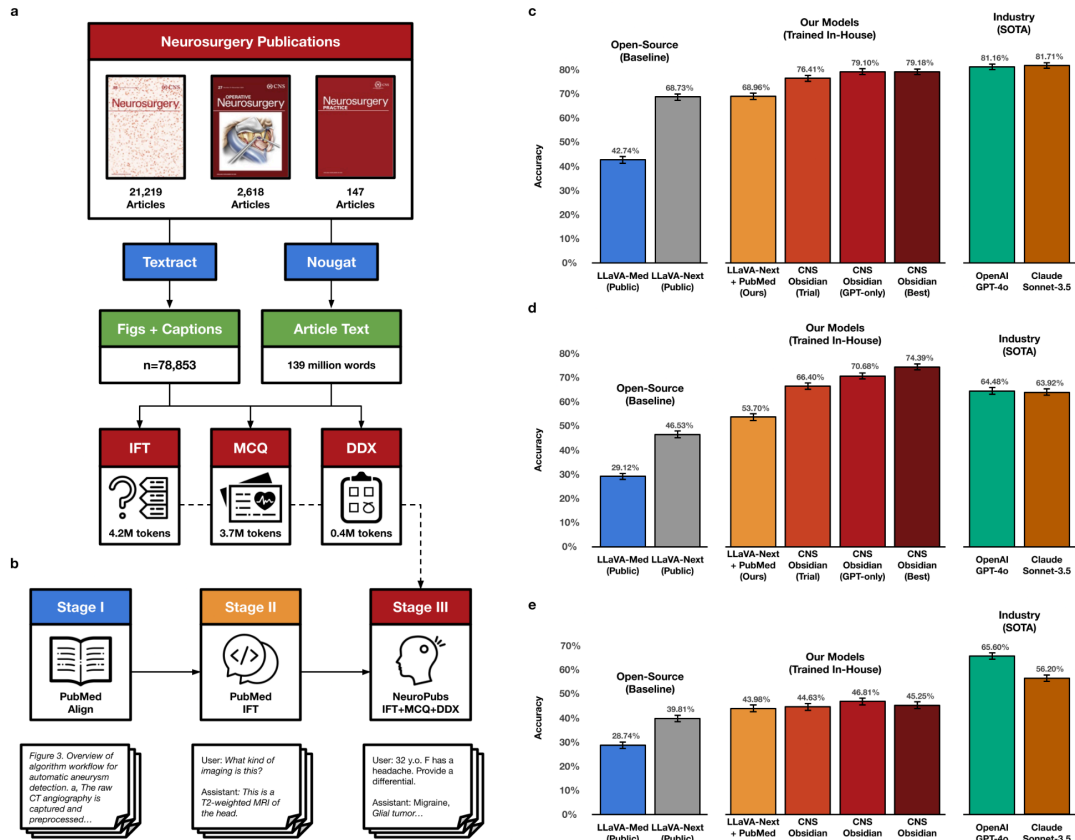


Fig. 3. Dataset, curriculum training, and benchmark performance. (A) Acquisition, processing, and knowledge translation pipeline for converting our specialty journal into an AI knowledge database (139 million words, 78,853 captioned figures) and subsequently into task-specific vision-language datasets. (B) Our approach includes a novel stage in training a medical specialty-specific (neurosurgical) VLM and to a downstream task (diagnosis) while preserving the conversation and question-answering capabilities of general models like ChatGPT. (C) MCQ performance on GPT-generated questions ($n=1,282$ questions) (D) MCQ performance on Claude-generated questions ($n=1,239$ questions) (E) MCQ performance on one-shot board-style questions ($n=950$ questions).

Note: Two-sided Fisher's exact tests were performed to assess differences in proportions (% accuracy) between models across benchmarking comparisons. Error bars represent standard error in all graphs.

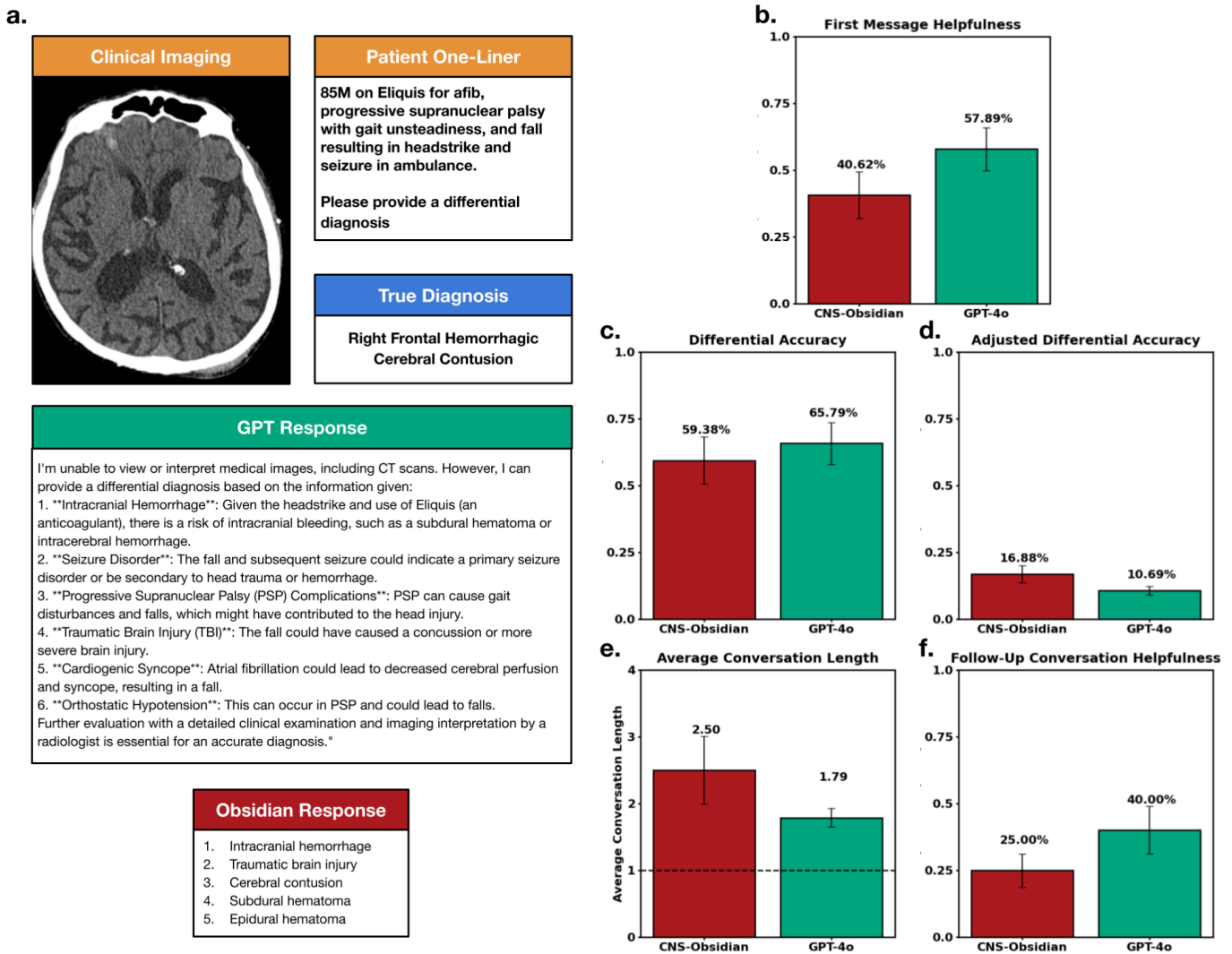


Fig. 4. Randomized controlled trial results. (A) A visual depiction of the workflow with a representative patient encounter. During the three-month trial, users interact with a web-based chat interface to interact with the VLM for differential diagnosis assistance (see Fig. S9 for interface details). The conversation is initialized by a neurosurgical resident who provides an image and a text input for evaluation (see Fig. S10 for interaction details). A single representative planar image (e.g., from X-ray, CT, MRI, or digitally captured photos of the pathology) is selected at the discretion of the neurosurgery trainee, as well as a brief one-liner statement summarizing pertinent elements of the patient history (e.g., age, sex, past medical history, medications, presenting symptoms). Upon prompting, GPT or CNS-Obsidian provides a text response with a tiered differential diagnosis. Outputs from GPT, counterfactual CNS-Obsidian output, and the actual diagnosis are shown. Compared to our CNS-Obsidian, GPT generated a broader but less specific set of diagnoses in a more conversational tone. (B) Diagnostic helpfulness of differential (user-rated) (C) Diagnostic accuracy of differential (AI-rated) (D) Diagnostic accuracy, adjusted for response length (E) Conversation length (F) Clinical helpfulness of follow-up chats (user-rated).

Note: For panels B-E, data represents n=32 for CNS-Obsidian and n=38 for GPT-4o. For panel F, data represents n=48 for CNS-Obsidian and n=30 for GPT-4o. Two-sided Fisher's exact tests were performed to assess differences in proportions (% upvote rate) between models in panels B, C, and F. Two-sided Mann-Whitney U tests were performed to assess differences in distributions (adjusted accuracy and conversation length) between models in panels D and E. Error bars represent standard error in all graphs.

Supplementary Figures

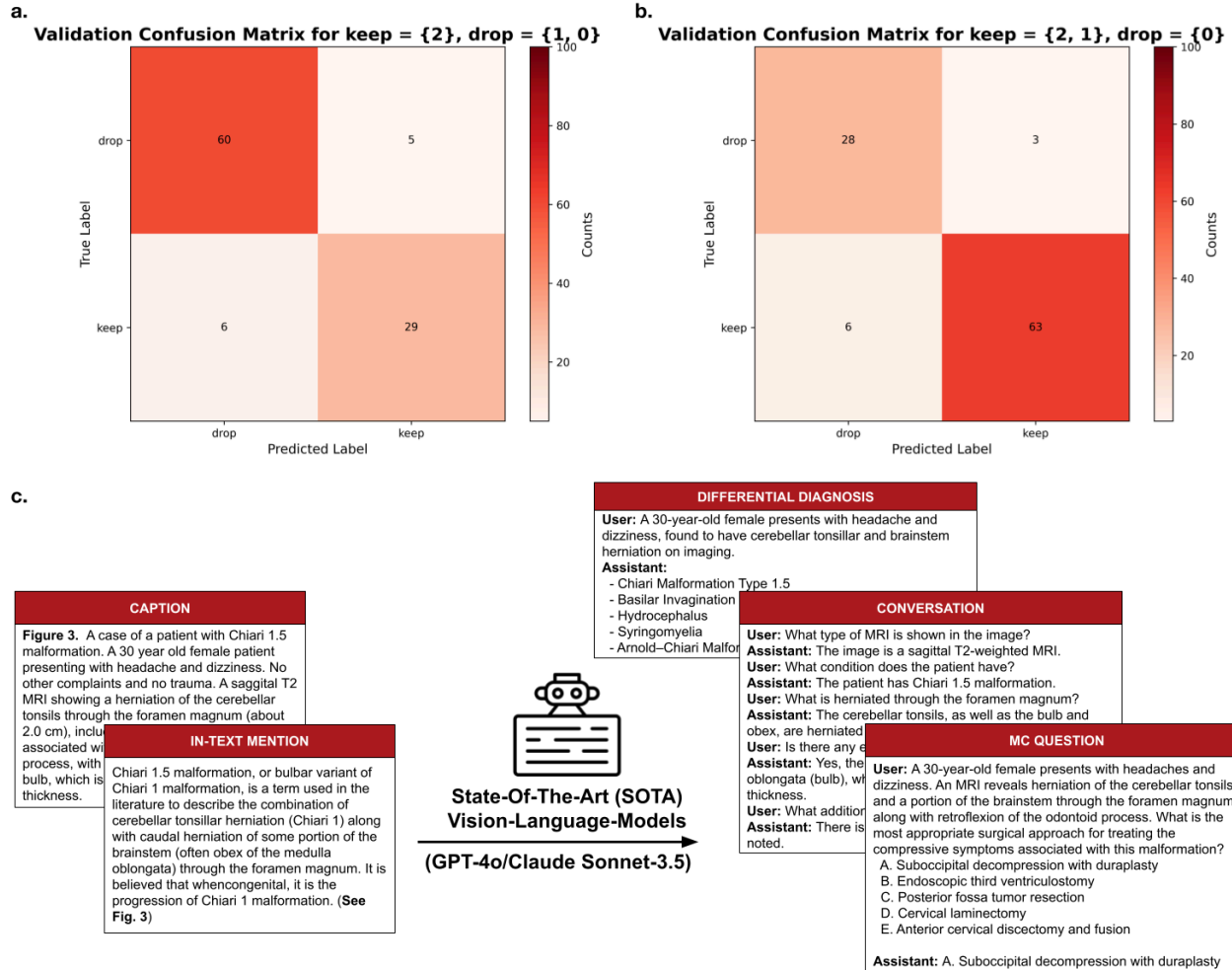


Fig. S1. Dataset filtering and knowledge translation pipeline. (A) Validation confusion matrix for the image content classification system when retaining Class 2 images (medical imaging: CT, MRI, X-ray, angiography) and filtering out Classes 1 (clinical visuals: surgical fields, microscopy, anatomical drawings) and 0 (technical content: flowcharts, survival curves, tables). Used to create the differential diagnosis dataset. (B) Validation confusion matrix for the classifier when retaining Classes 1 and 2 combined while filtering out Class 0. Used to create the multiple choice dataset. For both (A) and (B), the classifiers were based on ResNet-50 feature extraction and a linear classifier trained on 400 manually annotated images. Confusion matrices demonstrate validation performance on the held out 100 manually labeled images. (C) Knowledge translation pipeline demonstrated through conversion of neurosurgical data into training datasets. The example illustrates the automated conversion of specialized knowledge (figure, caption, in-text mention) into three distinct data formats: 1) natural instructional dialogue between user and assistant, 2) clinical vignette with multiple-choice options and detailed explanation, and 3) concise one-liner with prioritized differential diagnoses. The pipeline employs large language models (GPT-4o here) with few-shot in-context learning (four examples for each task randomly selected from pools of 10) to generate consistently formatted outputs while preserving diagnostic accuracy and educational value. Image: case courtesy of Rodrigo Dias Duarte, Radiopaedia.org, rID: 50409. Caption and in-text mention written based on the case information provided on Radiopaedia.org.

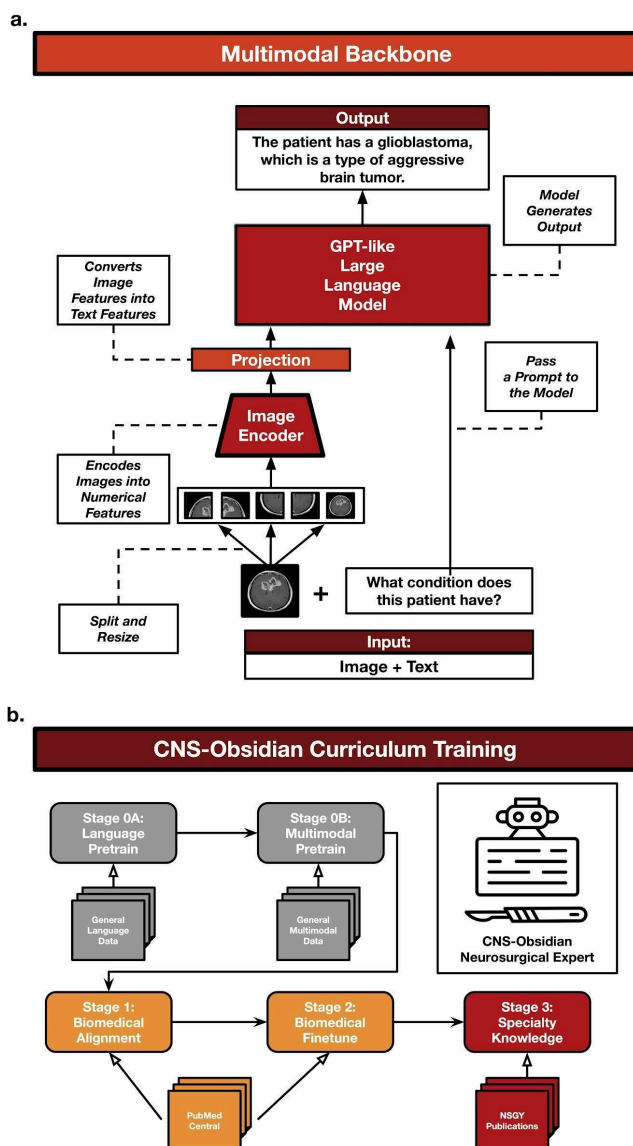


Fig. S2. Training a specialty vision-language model. (A) LLaVA-Next is a vision-language model that combines two modalities by slicing the high-resolution image into small patches and embedding them together with a resized full image. It then projects the visual features into the text space, and uses a pre-trained autoregressive model to generate output conditioned on both the image and the prompt. (B) A specialist model is trained in a stages, beginning with general language and multimodal pretraining (Stages 0A and 0B), followed by general medical alignment and finetuning (Stages 1 and 2), and culminating in specialty knowledge integration (Stage 3) using NeuroPubs. This curriculum-based approach was used to create CNS-Obsidian, a neurosurgical expert system capable of interpreting medical imaging and providing specialized diagnostic assessments.

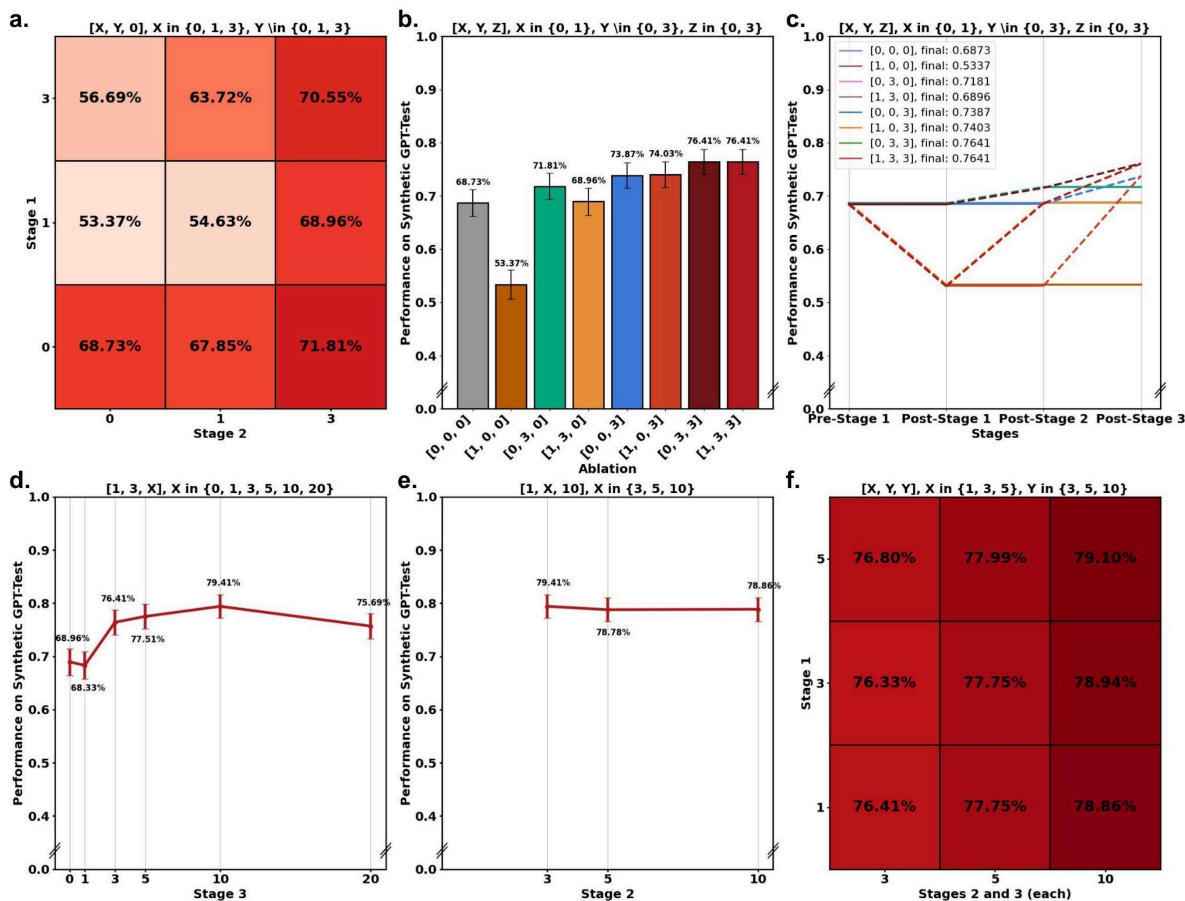


Fig. S3. Ablation studies of three-stage training using GPT-generated evaluations. Configuration $[X, Y, Z]$ denotes number of epochs in Stages 1, 2, and 3. (A) Impact of Stage 1 (alignment) and Stage 2 (general fine-tuning) epochs on model accuracy using GPT tgenerated MCQs dataset ($n=1,282$), with Stage 3 fixed at 0. Darker red indicates higher accuracy. Baseline $[0, 0, 0]$ achieves 68.73%. Alignment-only training shows performance degradation. (B) Performance comparison across configurations demonstrating each training stage's contribution. Error bars represent standard error. The full three-stage model $[1, 3, 3]$ achieves 76.41% accuracy, with Stage 3 contributing the largest improvement (+7.45%, $p<0.0001$). (C) Temporal evolution of model performance across training stages for different configurations. Solid lines represent measurements, dashed lines show interpolated trajectories. (D) Optimization of Stage 3 (task-specific fine-tuning) duration using configuration $[1, 3, X]$, where X varies from 0 to 20 epochs. Performance exhibits monotonic improvement until peaking at $X = 10$ epochs (79.48%). (E) Impact of Stage 2 duration on model performance using configuration $[1, X, 10]$, where X varies from 3 to 10 epochs. Performance remains stable across durations, $[1, 3, 10]$ achieving optimal performance (79.41%) on GPT generated MCQs and selected as one of final configuration candidates. (F) Joint optimization of Stage 1 and Stage 2/3 durations (configurations $[X, Y, Y]$). Longer fine-tuning stages show performance improvements. $[5, 10, 10]$ selected as one of the final configurations.

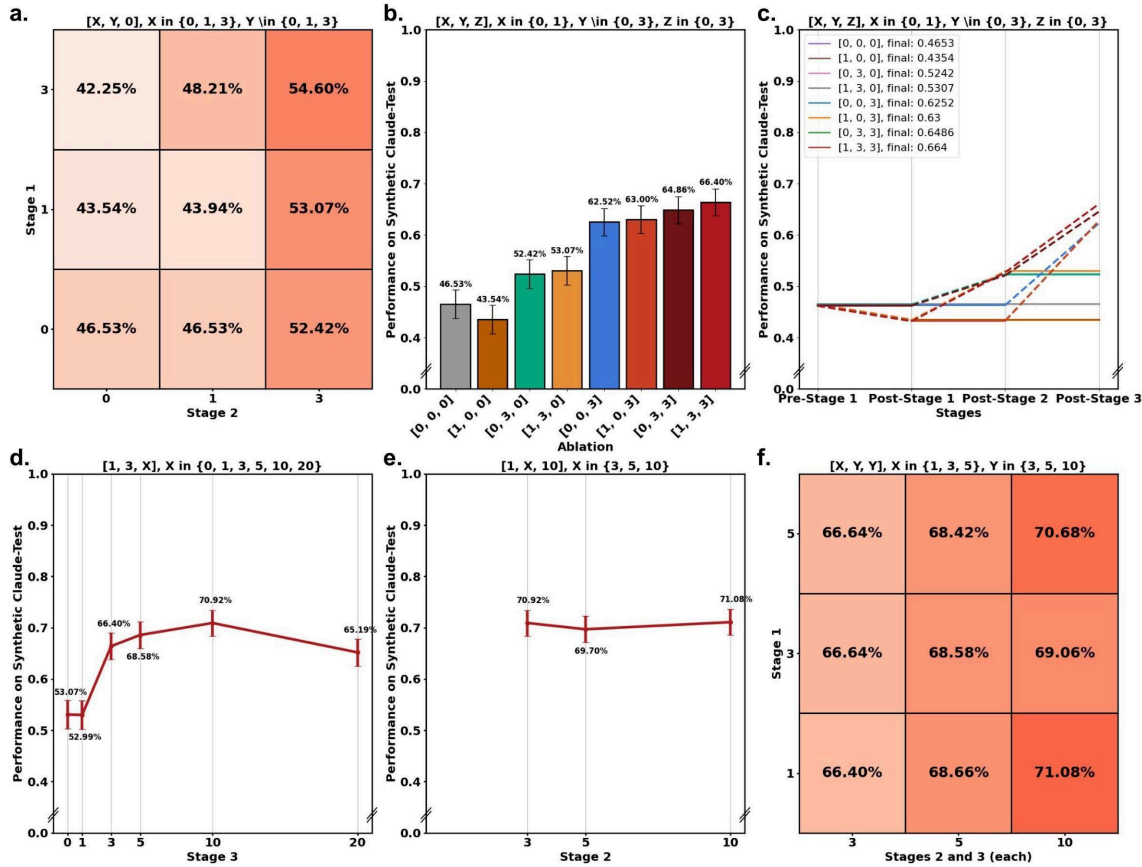


Fig. S4. Ablation studies of three-stage training using Claude-generated evaluations. Configuration $[X, Y, Z]$ denotes number of epochs in Stages 1, 2, and 3. (A) Impact of Stage 1 (alignment) and Stage 2 (general fine-tuning) epochs on model accuracy using Claude generated MCQs dataset ($n=1,239$), with Stage 3 fixed at 0. Darker red indicates higher accuracy. Baseline $[0, 0, 0]$ achieves 46.53%. Alignment-only training $[1, 0, 0]$ decreases performance to 43.54%. (B) Performance comparison across configurations showing each stage's contribution. Error bars represent standard error. The full three-stage model $[1, 3, 3]$ shows substantial improvement, with Stage 3 providing the largest gain (+13.33%, $p < 10^{-12}$). (C) Temporal evolution of model performance across training stages. Solid lines represent measurements, dashed lines show interpolated trajectories. (D) Optimization of Stage 3 duration using configuration $[1, 3, X]$. Performance peaks at $X = 10$ epochs (70.92%) before plateauing. (E) Effect of Stage 2 duration $[1, X, 10]$. Performance remains stable, with $[1, 10, 10]$ achieving slightly better results (71.08%, $p=0.9647$). (F) Joint optimization of Stage 1 and Stage 2/3 durations (configurations $[X, Y, Y]$). Longer training shows improvements, leading to selection of $[5, 10, 10]$ for final evaluation using both datasets.

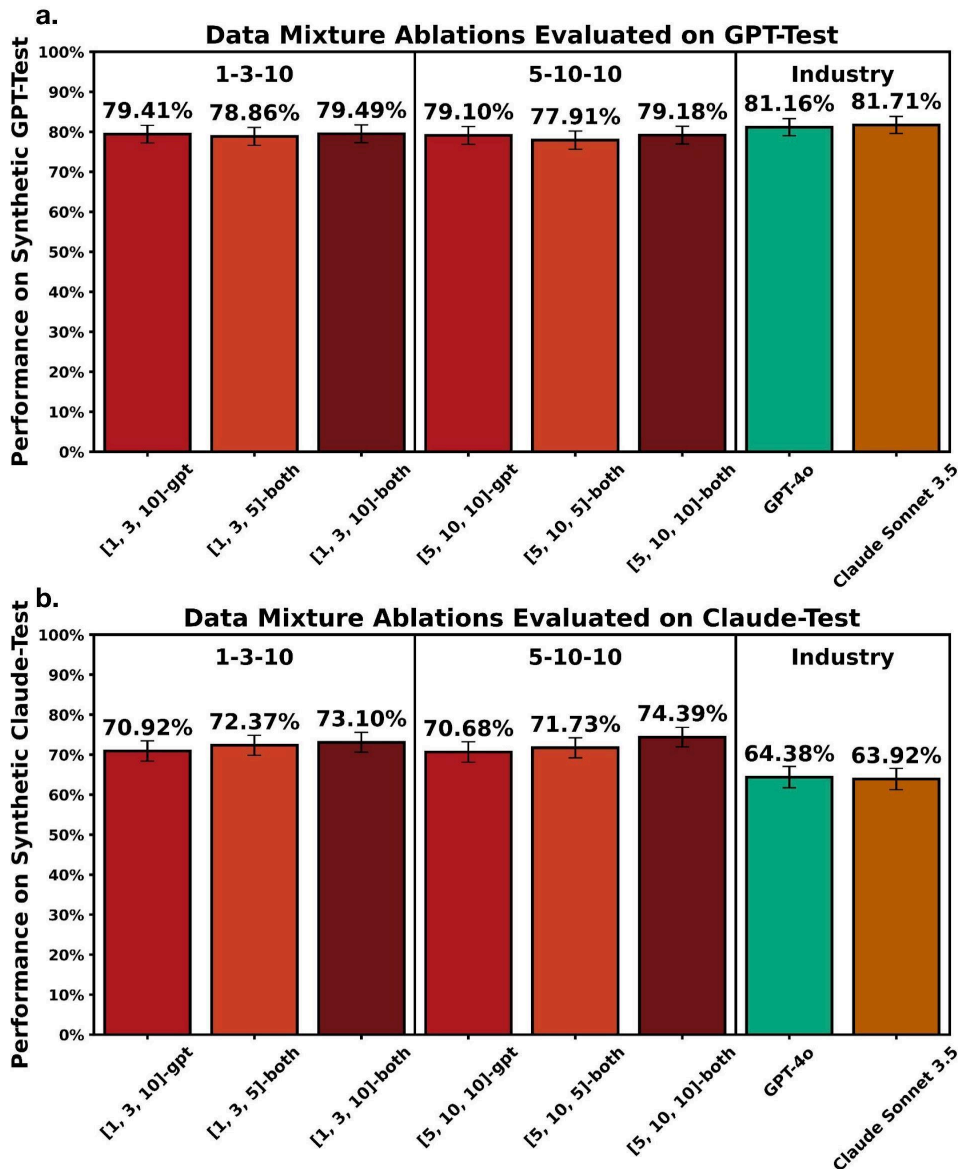


Fig. S5. Ablation experiments for data mixtures. (A) Performance on GPT generated MCQs ($n=1,282$) comparing models trained on GPT-generated data only (*-gpt*) versus both data sources (*-both*). Two base configurations $[1, 3, 10]$ and $[5, 10, 10]$ were each evaluated under two constraints when using both datasets: compute-matched (halved epochs) and epoch-matched (doubled compute due to doubled dataset). Including Claude-generated data showed no improvement over GPT-only training ($p=1.000$ for $[5, 10, 10]$ -*gpt* vs. $[5, 10, 10]$ -*both*). (B) Performance on Claude generated MCQs ($n=1,239$). Epoch-matched training on both datasets shows significant improvement ($p=0.0427$), with $[5, 10, 10]$ -*both* reaching 74.39% compared to baseline Claude Sonnet 3.5, 63.92%. In both evaluations, epoch-matched consistently outperforms compute-matched training. Error bars represent standard error.

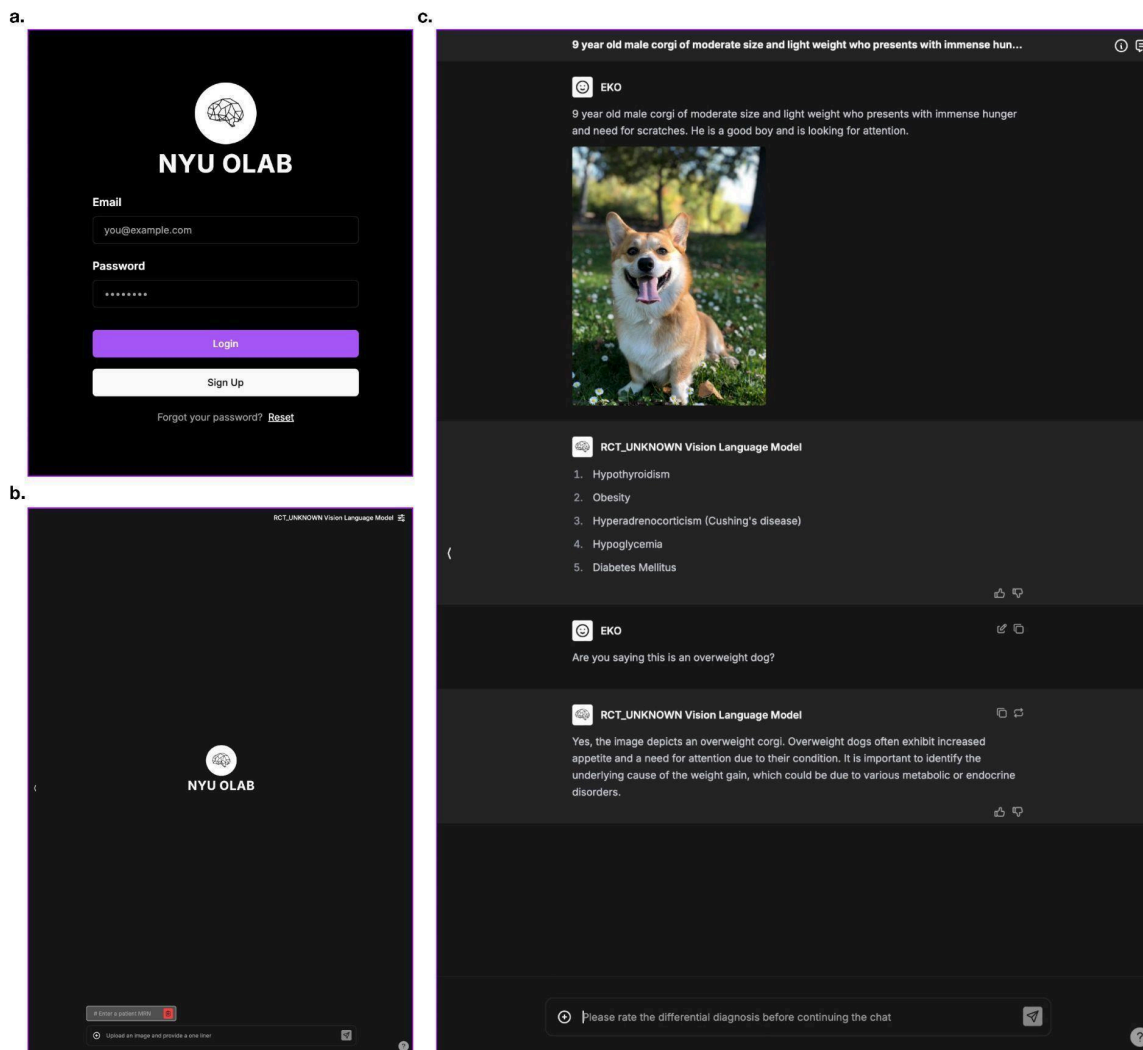


Fig. S6. Randomized controlled trial user interface. (A) The landing login interface. All participants had individual accounts with stored chat histories. Access was manually curated by the team. (B) Post-login, the participants are directly forwarded to the chatbot interface which is designed to mimic the typical chatbot interfaces, but enhanced with randomized back-end, a patient MRN field, and an ability to submit an image, including via intuitive “drag-and-drop”. (C) An example interaction with the model. The users can provide binary feedback for individual messages using “upvote” and “downvote” buttons. The model interacted with for this chat is CNS-Obsidian, but the participants are blinded to this information.

😊

This is a 50 year old man presenting to ER with acute paraplegia. He's on warfarin.



🧠 RCT_UNKNOWN Vision Language Model

1. Spinal epidural hematoma
2. Spinal cord compression
3. Spinal arteriovenous malformation
4. Intramedullary spinal tumor
5. Spinal abscess

👍 🗨️

😊

Which of these is it most likely?

🧠 RCT_UNKNOWN Vision Language Model

Given the patient's presentation of acute paraplegia and the imaging findings of a hyperintense lesion in the spinal cord on T2-weighted MRI, the most likely diagnosis is a spinal epidural hematoma. This condition is characterized by rapid onset of symptoms due to the acute compression of the spinal cord by a hematoma. The patient's use of warfarin further supports this diagnosis as it can predispose to spontaneous bleeding. Other conditions like spinal cord compression, spinal arteriovenous malformation, intramedullary spinal tumor, and spinal abscess may present similarly but are less likely given the acute presentation and the use of anticoagulants. A detailed clinical history, imaging findings, and neurological examination will help confirm the diagnosis and guide management.

👍 🗨️

😊

What is the treatment?

🧠 RCT_UNKNOWN Vision Language Model

The treatment for a spinal epidural hematoma typically involves urgent surgical intervention to evacuate the hematoma and relieve the compression on the spinal cord. This is to prevent further neurological deterioration and to restore neurological function. Immediate discontinuation of anticoagulant therapy such as warfarin is also necessary to prevent further bleeding. Postoperatively, careful monitoring of neurological status, pain management, and rehabilitation are crucial for optimal recovery. Management of the underlying cause of the bleeding, such as stopping anticoagulation or addressing a bleeding disorder, is also important.

👍 🗨️

⊕ Please rate the differential diagnosis before continuing the chat 🗨️

Fig. S7. An example patient submitted to the study interface. Identifying details anonymized. The model interacted with is CNS-Obsidian-base (version actually used in the trial). For more examples of a base and final model see **Movie S1** and **Movie S2**, respectively.

Supplementary Results

Ablation Experiments

Notation

We denote experimental configurations as $[X, Y, Z]$, where X , Y , and Z represent the number of epochs in Stage 1 (alignment), Stage 2 (general fine-tuning), and Stage 3 (task-specific fine-tuning), respectively. Performance metrics are reported on two held-out test sets: GPT-Test ($n=1,282$ questions) and Claude-Test ($n=1,239$ questions). Due to the paper-level split we respected, no model has seen any figure from the same paper as any of the held out test questions. Most of our models are trained only on the data converted from the NeuroPubs using GPT-4o only. We refer to these models as $[X, Y, Z]$ -gpt, or $[X, Y, Z]$ for brevity. We also conducted ablations and experiments that used data converted via both GPT and Claude; those models will be explicitly referred to $[X, Y, Z]$ -both.

LLaVa-Next-Med Ablations

We first validated our three-stage training approach on LLaVA-Next-Med by systematically varying Stage 1 and Stage 2 epochs while maintaining Stage 3 = 0. The baseline configuration $[0, 0, 0]$ achieved 68.73% accuracy on GPT-Test and 46.53% on Claude-Test. Alignment-only training ($[1, 0, 0]$) decreased performance to 53.37% on GPT-Test and 43.54% on Claude-Test, indicating degradation of instruction-following capabilities. Stage 2 training improved performance, with $[0, 3, 0]$ achieving 71.81% on GPT-Test and $[3, 3, 0]$ reaching 54.60% on Claude-Test.

CNS-Obsidian Missing Stages Ablations

We then considered adding 3 epochs of Stage 3 to the $[1, 3, 0]$ model (the length used by LLaVA-Med), making the $[1, 3, 3]$ model, which served as our base CNS-Obsidian. To evaluate the contribution of each training stage, we conducted comprehensive ablation experiments on CNS-Obsidian by systematically removing different stages. We tested eight configurations: $[0, 0, 0]$, $[1, 0, 0]$, $[0, 3, 0]$, $[1, 3, 0]$, $[0, 0, 3]$, $[1, 0, 3]$, $[0, 3, 3]$, and $[1, 3, 3]$. On GPT-Test the baseline $[0, 0, 0]$ achieved 68.73%, while the full three-stage model $[1, 3, 3]$ reached 76.41%, representing an 11.18% relative improvement. Inclusion of Stage 3, the neurosurgical specialization, leads to an improvement of +7.45% on GPT-Test ($p < 0.0001$) and +13.33% on Claude-test ($p < 10^{-12}$). The impact of Stage 2 (general medicine integration) was similarly present, but modest with +2.38% ($p=0.1848$) and +3.40% ($p=0.0522$) improvements on GPT-Test and Claude-Test, respectively. Lastly, the inclusion of Stage 1 alignment did not affect performance on GPT-Test, but boosted the performance on Claude-Test by +1.54% ($p=0.3994$). These results confirm the complementary nature of all training stages.

Optimization of Task-Specific Fine-Tuning

We investigated the optimal duration of task-specific fine-tuning (Stage 3) by evaluating configurations $[1, 3, X]$ where $X \in \{0, 1, 3, 5, 10, 20\}$. Performance exhibited a monotonic improvement until $X = 10$, with the model achieving peak performance on both GPT-Test (79.48%) and Claude-Test (70.92%). Training beyond 10 epochs led to performance plateauing and slight decreases.

General Fine-Tuning Duration Analysis

To optimize Stage 2, we evaluated configurations $[1, X, 10]$ where $X \in \{3, 5, 10\}$. Remarkably, performance remained stable across different Stage 2 durations. For GPT-Test the best-performing checkpoint of these was $[1, 3, 10]$ at 79.41%. For Claude-Test the $[1, 10, 10]$ slightly outperformed the other two models at 71.08%. Notably, the differences between the two were not statistically significant on both GPT-Test ($p=0.8079$) and Claude-Test ($p=0.9647$). We decided to use $[1, 3, 10]$ as one of the checkpoints to retrain using both datasets, but also to evaluate different training lengths of checkpoint that have the same number of Stages 2 and 3.

Comprehensive Stage Length Optimization

Our final experimental series explored the joint optimization of alignment and fine-tuning stages through configurations $[X, Y, Y]$ where $X \in \{1, 3, 5\}$ and $Y \in \{3, 5, 10\}$. Overall, we observed an expected pattern of improvements with longer fine-tuning stages. The changes between the alignment length were not significant, but generally leaned towards better performance with longer training, at least on GPT-Synth, so we picked $[5, 10, 10]$ as the other candidate to be retrained with both GPT and on both datasets.

Secondary Data Source

To maximize model performance, we evaluated our top configurations ($[1, 3, 10]$ and $[5, 10, 10]$) using data processed by both GPT and Claude. $[5, 10, 10]$ -both achieved 79.18% on GPT-Test and 74.39% on Claude-Test. For comparison, GPT-4o achieved 81.16% on GPT-Test and Claude Sonnet 3.5 reached 63.92% on Claude-Test.

Obsidian RCT Written User Manual

Title of Study:	NYUConsult: A General Medical AI Chatbot 23-00510
Principal Investigator:	Eric Oermann, MD Department of Neurosurgery NYU Langone Health 530 1 st Avenue, Suite 8S, New York, New York 10016
Emergency Contact:	Eric Oermann, MD

Introduction

You are to evaluate a chatbot created by the **NYU Langone Department of Neurosurgery** for its ability to **provide differential diagnoses, answer follow-up questions, and interpret medical imaging**.

You will provide the chatbot with a patient MRN, the most significant medical image for the case, and a brief clinical summary (“one-liner”). The chatbot will provide a differential diagnosis, which you will approve or disapprove. You can then continue asking questions or discussing the case if you would like, and rating those interactions as desired.

Your task is to interact with the system by reviewing the chatbot's differential diagnosis, asking follow-up questions, and evaluating the responses. You will assess whether or not the differential diagnosis and any follow-up is clinically helpful. The goal is to compare the performance of the NYU chatbot against the PHI-safe GPT-4o in medical diagnosis and consultation tasks. You will use an interface that randomly selects which chatbot you interact with for each new conversation.

Network Requirement

You must be on the NYU network (at Tisch/Kimmel) to access the chatbot (sorry, Bellevue and VA crew).

AI Diagnostic Chatbot Setup

1. Login to the web app at <http://10.189.26.12:31111/>
2. Click on **Sign Up** and create a new account using your NYU Langone e-mail address.
3. Contact jayden.stryker@nyulangone.org if you are having issues setting up your account.


NYU OLAB

Email

Password

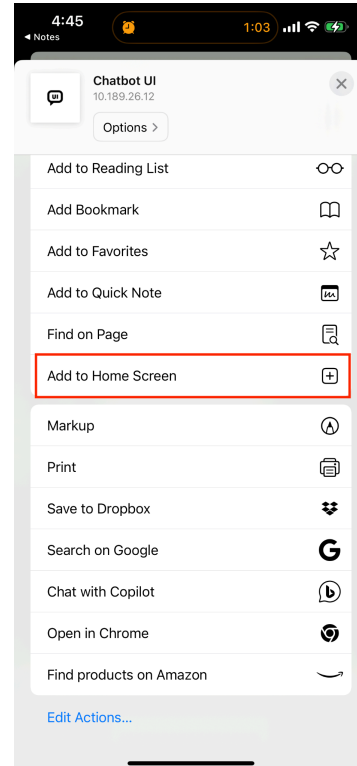
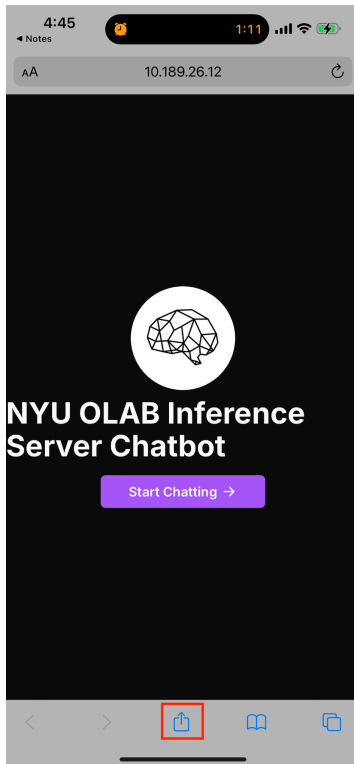
[Login](#)

[Sign Up](#)

Forgot your password? [Reset](#)

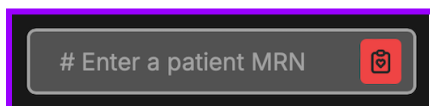
Add to Home Screen for Easy Access as a Web App

1. Go to the link above on your iPhone and select the Share button at the bottom.
2. Then click on **Add to Home Screen** to add it as a Web Application on the Home screen of your iPhone for easy access.

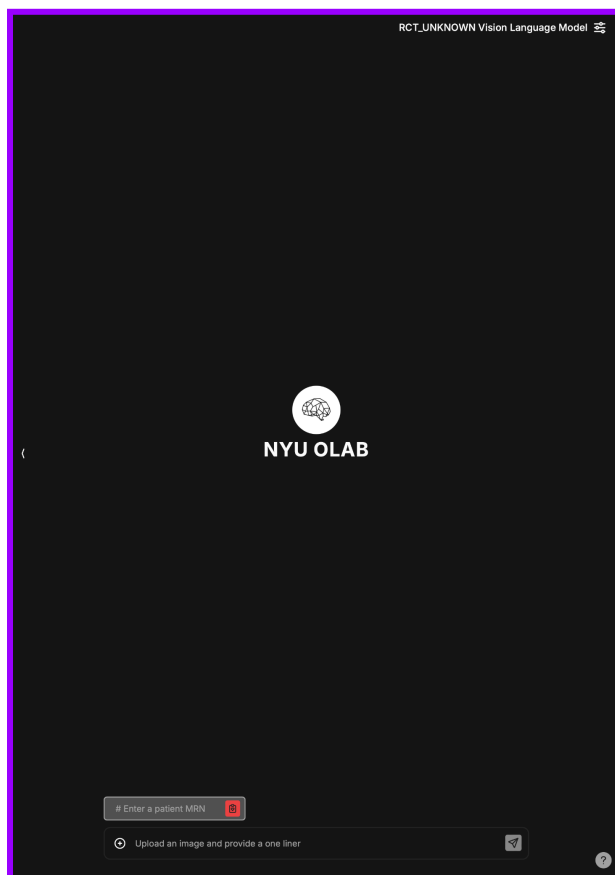


Step-by-step Instructions to use

1. Log into the app. The interface is similar to ChatGPT.
2. Start a new chat with **RCT_UNKNOWN Vision Language Model**.
3. For your current patient in clinic, pre-op, or as a new consult, think of a one-liner for the patient that summarizes their basic presentation, HPI, and findings. **Do not include their diagnosis if it is known**. Also identify the single most important visual image for the case (a MRI slice, a picture of the telemetry, a wound, etc...).
4. Enter the information into the chat.
 - a. First enter the **[MRN]** in the grey box above the chat window.



- b. Then click on the  button and upload an image from your phone or computer (see below for guidance on choosing good images).
 - c. Lastly, enter a one-liner into the chat window and click on the send button  to get a differential diagnosis and initiate a chat. **A 67-year-old male with a past medical history of hypertension, is brought in by EMS. He is hypertensive with a SBP in the 160s, tachycardic, and is obtunded with a GCS of 3T.**
5. The model will output a *differential diagnosis* of the case.
 - a. Please click on **Thumbs Up**  if, in your clinical opinion, the model's outputs are **helpful**.
 - b. Please click on **Thumbs Down**  if, in your clinical opinion, the model's outputs are **unhelpful**.
 - c. **Please do not skip this step, as it is the primary outcome measure of our study.**
6. You can continue to chat with the model if you like. It should be able to answer basic questions about neurosurgical care and diagnostics. If you like or dislike the follow-up messages, please rate them as you see fit (see sample conversation below about a Corgi).



9 year old male corgi of moderate size and light weight who presents with immense hun... ⓘ 🗨️

 EKO

9 year old male corgi of moderate size and light weight who presents with immense hunger and need for scratches. He is a good boy and is looking for attention.



 RCT_UNKNOWN Vision Language Model

1. Hypothyroidism
2. Obesity
3. Hyperadrenocorticism (Cushing's disease)
4. Hypoglycemia
5. Diabetes Mellitus

👍 🗨️

 EKO ✍️ 📄

Are you saying this is an overweight dog?

 RCT_UNKNOWN Vision Language Model 📄 🗨️

Yes, the image depicts an overweight corgi. Overweight dogs often exhibit increased appetite and a need for attention due to their condition. It is important to identify the underlying cause of the weight gain, which could be due to various metabolic or endocrine disorders.

👍 🗨️

🔄 Please rate the differential diagnosis before continuing the chat 🗨️ ?

7. When you are done, create a new chat before starting another patient's case.
- a. The button in the top right corner  can do this quickly.
 - b. You can also use the chat log on the left. .
 - c. **EVERY PATIENT MUST HAVE THEIR OWN CHAT**

TIPS

Image Guidelines

Pick the most significant image relevant to the case. Think of what visual you might include in a case report about the patient. Some examples include:

- Slice of a CT/MRI
- Picture of a wound
- Picture of telemetry recording

You can take a screenshot of a PACS or other image on your phone or use an image directly from your phone camera (e.g., of a wound/dressing).

Please avoid using photos taken of a computer monitor. The glare will make it difficult to interpret and artificially deflate performance. Again, consider what you might present at grand rounds or in a case report. Think of what image you'd want to include as your main visual in a case report, and try to present it that way. For example, for an elderly male with a new cerebellar metastasis, we might want a slice from their CT:



Note how the image is cropped from the full Visage screenshot (below) to make it more presentable.

ONE-LINER Guidelines

This is a one-liner presentation of the patient's clinical situation when you encounter them. It should reference the core aspects of their neurosurgical presentation, again, **think of how a rapid presentation would go during patient handoff.**

Troubleshooting / Contact

If you have any questions, please email anton.alyakin@nyulangone.org, jayden.stryker@nyulangone.org, or eric.oermann@nyulangone.org. Also, feel free to text Dr. Oermann anytime (you all have his number).